Pilot-Wave Hydrodynamics

John W.M. Bush

Department of Mathematics, Massachusetts Institute of Technology, Cambridge,
Massachusetts 02139; email: bush@math.mit.edu

Keywords

walking drops, Faraday waves, quantum analogs

Abstract

Yves Couder, Emmanuel Fort, and coworkers recently discovered that a
millimetric droplet sustained on the surface of a vibrating fluid bath may
self-propel through a resonant interaction with its own wave field. This ar-
ticle reviews experimental evidence indicating that the walking droplets ex-
hibit certain features previously thought to be exclusive to the microscopic,
quantum realm. It then reviews theoretical descriptions of this hydrody-
namic pilot-wave system that yield insight into the origins of its quantum-
like behavior. Quantization arises from the dynamic constraint imposed
on the droplet by its pilot-wave field, and multimodal statistics appear to
be a feature of chaotic pilot-wave dynamics. I attempt to assess the po-
tential and limitations of this hydrodynamic system as a quantum analog.
This fluid system is compared to quantum pilot-wave theories, shown to
be markedly different from Bohmian mechanics and more closely related to
de Broglie's original conception of quantum dynamics, his double-solution
theory, and its relatively recent extensions through researchers in stochastic
electrodynamics.

1. INTRODUCTION

> Long may Louis de Broglie continue to inspire those who suspect that what is proved by impossibility proofs is lack of imagination.
>
> J.S. Bell (1982)

Both fluid dynamics and quantum mechanics attempt to describe the motion of particles and waves in continuous media, albeit on vastly different scales. Given the relative familiarity and accessibility of fluid systems, it is only natural to draw analogies with them as one attempts to come to grips with the oddities of quantum mechanics. Newton (1979) described photons skipping through the ether like stones on the surface of a pond. Young (1804) demonstrated the wave nature of light via analogy with ripple tank experiments. Berry et al. (1980) examined plane waves sweeping over a vortex as a hydrodynamic analog of the Aharonov-Bohm effect (Coste et al. 1999). A recent hydrodynamic analog of the Casimir effect suggests that Faraday waves can mimic the role of vacuum fluctuations in generating forces between neighboring objects (Denardo et al. 2009). The theories of fluid and quantum mechanics converge in the realm of superfluids (Donnelly 1993) and Bose-Einstein condensates (Pitaevskii & Stringari 2003). The first hydrodynamic analogs of single-particle quantum systems have emerged in the past decade from the Paris laboratory of Yves Couder.

When placed on a vibrating fluid bath, a millimetric drop may interact with the surface in such a way as to walk steadily across it at a characteristic speed of 1 cm/s, guided or piloted by its own wave field (Couder et al. 2005b, Protière et al. 2006) (**Figure 1***c*). The resulting walkers are spatially extended objects comprising both the droplet and wave (Eddi et al. 2011b). By virtue of their spatial delocalization, they exhibit several features previously thought to be peculiar to the microscopic quantum realm (Bush 2010). Specifically, the walkers exhibit behavior reminiscent of single-particle diffraction (Couder & Fort 2006), tunneling (Eddi et al. 2009b), quantized orbits (Fort et al. 2010, Harris & Bush 2014a, Perrard et al. 2014a,b), orbital level splitting (Eddi et al. 2012, Oza et al. 2014a), and spin states (Oza et al. 2014a). Coherent, multimodal statistics have been observed to emerge in single-particle diffraction (Couder & Fort 2006), motion in confined geometries (Harris et al. 2013), orbital motion in a rotating frame (Harris & Bush 2014a), and orbital motion in a central force (Perrard et al. 2014a,b). The basic mechanics and quantum-like features of the walker system are reviewed in Section 2. The theoretical models developed to rationalize the walker dynamics are reviewed in Section 3.

Section 4 explores the relation between this fluid system and realist descriptions of quantum systems, the majority of which are rooted in the hydrodynamic formulation of quantum mechanics (Madelung 1926). The walker system bears a notable resemblance to an early conception of relativistic quantum dynamics, Louis de Broglie's (1926, 1930, 1956, 1987) double-solution
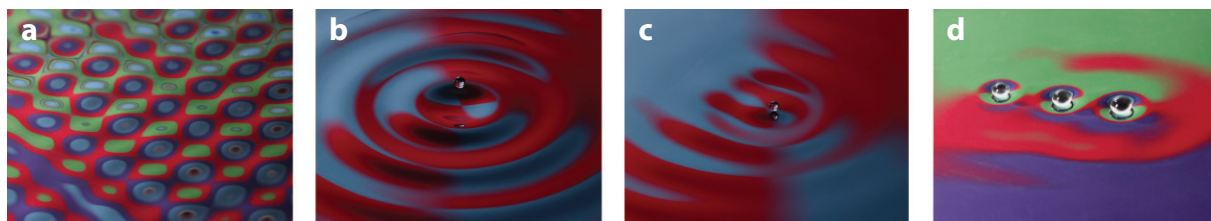

Figure 1

Image gallery of (*a*) Faraday waves, just above threshold; (*b*) a bouncing drop; (*c*) a walker; and (*d*) a trio of bouncers. Photographs courtesy of Dan Harris.

pilot-wave theory, according to which microscopic particles move in resonance with their own wave field. The extensions of de Broglie's mechanics through researchers in stochastic electrodynamics (SED) (Kracklauer 1992, de la Peña & Cetto 1996, Haisch & Rueda 2000) are also touched on, and their relation to the walker system is discussed. Although this review is written from the perspective and in the language of a fluid mechanician, my hope is that it will encourage interest in revisiting and reappraising realist quantum theories from the fluid dynamics community and beyond.

2. WALKING DROPLETS

The phenomena of interest arise when a millimetric drop is levitated on the surface of a vibrating fluid bath (Walker 1978) (**Figure 1**), an understanding of which requires familiarity with both noncoalescence phenomena (Neitzel & Dell'Aversana 2002) and Faraday waves (Miles & Henderson 1990).

2.1. The Faraday Levitator

Casual observation indicates that water drops may skip across the water surface (Jayaratne & Mason 1964). The drop bounces if the collision time is less than the time taken for the intervening air layer to drain to the thickness at which coalescence is initiated by the attractive van der Waals forces acting between the drop and bath. Although this critical thickness generally depends on the liquid and gas phase properties, as well as the system cleanliness, it is typically ~100 nm (Couder et al. 2005a; Terwagne et al. 2007, 2009). In the case of rebound, the air layer communicates lubrication stresses (Reynolds 1886) between the drop and bath, causing the drop to deform, decelerate, and reverse direction (Gilet et al. 2007, Gilet & Bush 2012).

Let us consider a fluid of density ρ, kinematic viscosity ν, and surface tension σ in a horizontal bath of depth H, driven by a vertical vibration of amplitude A_0 and frequency $f = \omega/(2\pi)$. The effective gravity in the bath's frame of reference is $g + \gamma \sin \omega t$, where g is the gravitational acceleration and $\gamma = A_0 \omega^2$. At low γ, the fluid remains quiescent; however, above the Faraday threshold γ_F, the layer becomes unstable to a field of Faraday waves (Faraday 1831) (**Figure 1a**). The frequencies of the resulting waves are quantized, being integer multiples of half the driving frequency (Benjamin & Ursell 1954). Although higher harmonics may be excited, for the silicone oils used in the walker system, the most unstable waves are subharmonic, with half the frequency of the imposed vibrational forcing, $\omega_F = \omega/2$ (Douady 1990, Edwards & Fauve 1994, Kumar & Tuckerman 1994, Kumar 1996). Thus, as γ_F is crossed from below, the first waves to appear are subharmonic, with a wavelength $\lambda_F = 2\pi/k_F$ prescribed by the water-wave dispersion relation: $\omega_F^2 = (g k_F + \sigma k_F^3/\rho) \tanh k_F H$. The experimental system comprises a bath of silicone oil ($\nu \sim 10-100$ cS, $H \sim 4-10$ mm) subject to vertical vibrations ($f \sim 20-150$ Hz, $A_0 \sim 0.1-1$ mm) that induce vibrational accelerations $\gamma \leq 5g$ and wavelengths $\lambda_F \sim 3-10$ mm. For $f \geq 80$ Hz and $H \geq 7$ mm, the Faraday waves are effectively deep-water capillary waves with the dispersion relation $\omega_F^2 = \sigma k_F^3/\rho$.

The walker experiments are performed for $\gamma < \gamma_F$, so the fluid interface would remain flat in the absence of the drop; nevertheless, the Faraday forcing is critical. First, it powers the system, providing the energy for both the droplet motion and the resulting wave field. Second, it preconditions the bath for a monochromatic wave field. Eddi et al. (2011b) characterized the form of the wave field generated by particle impact on a vibrating bath ($\gamma < \gamma_F$) using a free-surface synthetic schlieren technique (Moisy et al. 2009). Following impact, a transient wave propagates away from the impact site at a speed of ~6 cm/s, and in its wake persists a field of standing Faraday waves,

whose longevity depends on the proximity to the Faraday threshold. A demonstration of walking drops may be simply realized using a petri dish glued onto a woofer from a loudspeaker. Drops of the desired size (diameter $D \sim 0.6-1.0$ mm) may be produced by breaking the interface with a toothpick. Illuminating with a strobe light makes for a striking demonstration.

Precision experiments require careful leveling and control of the vibrational forcing (Goldman 2002, Harris & Bush 2014b). Any variation from level, nonuniform vibration or spurious resonance results in a spatial dependence of the Faraday threshold. The walker dynamics and statistics are highly sensitive to all the system parameters, drop size, fluid properties, and forcing; consequently, repeatable experiments require the simultaneous control and documentation of each. Studies of the walker statistics are typically performed just below the Faraday threshold (Couder & Fort 2006, Harris et al. 2013, Harris & Bush 2014a, Perrard et al. 2014a,b). The duration of the experiments is thus limited by the constancy of the lab temperature, changes in which alter the Faraday threshold through the concomitant change in viscosity (Bechhoeffer et al. 1995). The bath should be covered with a fixed lid to eliminate air currents, a signature of which is curved rather than straight walker trajectories. Another concern in gathering reliable statistical data is the longevity of the droplet (Terwagne et al. 2007). Even in a controlled environment, rogue coalescence events arise, with a period on the order of an hour, presumably owing to the settling of impurities onto the bath. Such interruptions make clear the value of a mechanism for creating identical droplets on demand (Yang et al. 1997, Terwagne 2012).

Couder's group characterized the drop's bouncing behavior in terms of the drop diameter $D = 2a$ and dimensionless forcing acceleration γ/g (Protière et al. 2005), with viscosity-frequency combinations of 50 cS–50 Hz (Protière et al. 2006) and 20 cS–80 Hz (Eddi et al. 2008). Moláček & Bush (2013a,b) and Wind-Willassen et al. (2013) extended these studies to guide their theoretical developments. They introduced the vibration number, $V_i = \omega\sqrt{\rho a^3/\sigma}$, the relative magnitude of the forcing frequency and the drop's natural oscillation frequency, and characterized the droplet behavior in the $V_i - \gamma/g$ plane for various viscosity-frequency combinations. **Figure 2** presents a synthesis of their results for the 20 cS–80 Hz combination, which exhibits the most extensive walking regime. This presentation highlights a key feature of the system: A droplet most readily bounces or walks when forced at its natural frequency, when $V_i \approx 0.65$. Different bouncing states are denoted by (m, n), where m/f indicates the period of the bouncing mode, during which the drop contacts the surface n times.

Below the bouncing threshold, the drop coalesces into the bath. Just above it, bouncing arises in the $(1, 1)$ mode: The drop hits the bath once per driving period. Increasing the acceleration then leads to a $(2, 2)$ bouncing mode, in which the drop repeats a pair of bounces of unequal height. For relatively small and large drops, a period-doubling cascade may follow, culminating in chaotic bouncing or walking. For drops within a limited size range, typically 0.6 mm $< D <$ 1.0 mm, a period-doubled $(2, 1)$ bouncing mode emerges and then destabilizes into a $(2, 1)$ walker at the walking threshold γ_w. These $(2, 1)$ walkers bounce in synchrony with their monochromatic Faraday wave field, the underlying fluid behaving like a damped oscillator forced at resonance. However, more complex gaits may also arise within the walking regime, including mode-switching and chaotic walkers (Wind-Willassen et al. 2013). Section 3 reviews the theoretical rationale for this behavior.

2.2. New Classical Behavior

A critical feature of the walker system is that of path memory (Eddi et al. 2011b). The walker receives a lateral force at impact that depends on the local slope of the interface (Protière et al. 2006), whose form depends in turn on the previous impacts (Eddi et al. 2011b). In the low-memory
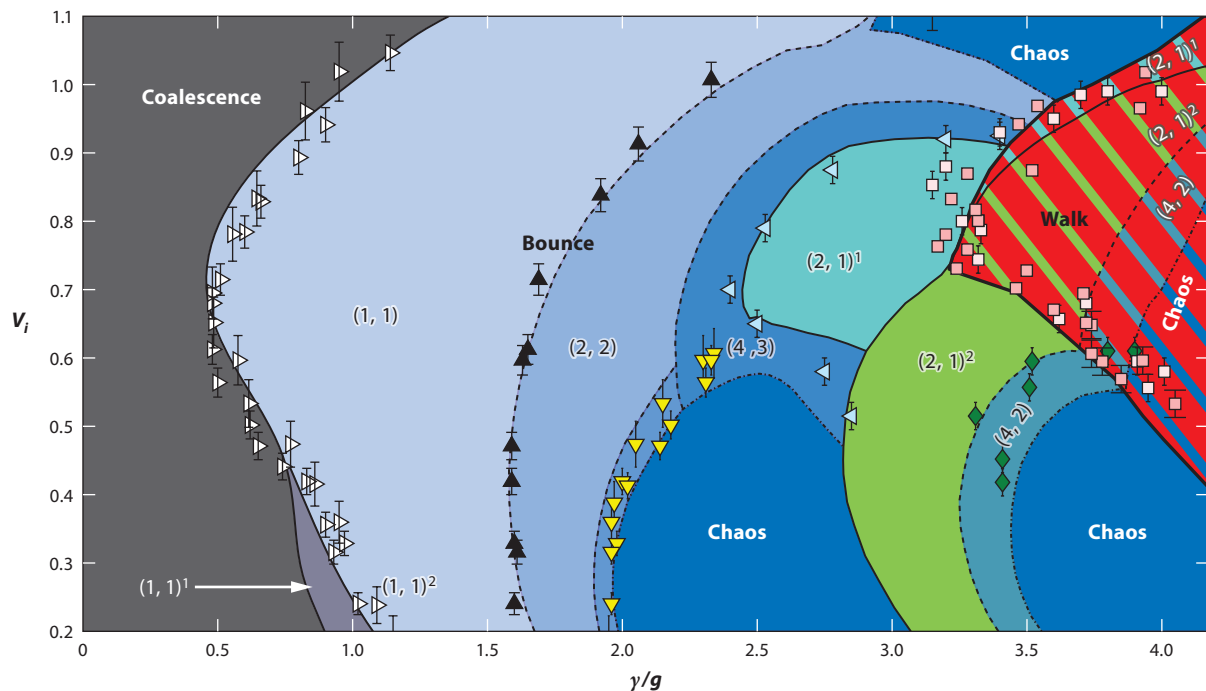
Figure 2

Regime diagram indicating the dependence of the drop's bouncing behavior on the driving acceleration, γ/g, and vibration number, $V_i = \omega/\sqrt{\sigma/\rho a^3}$. The fluid bath is 20-cS silicone oil driven at $f = \omega/2\pi = 80$ Hz. The associated Faraday threshold is $\gamma_F/g = 4.2$. A drop in the $(m, n)^i$ mode bounces n times in m forcing periods, with the integer subscript i ordering multiple (m, n) states according to their total mechanical energy, with $i = 1$ being the lowest. Colors indicate predicted bouncing and walking modes; data indicate measured thresholds between them (Moláček & Bush 2013b, Wind-Willassen et al. 2013).

limit, the waves are quickly damped, and the walker feels only the wave from its most recent impact. At high memory, the waves are relatively persistent, and the walker's trajectory depends on its distant past. Although this physical picture is quantified by the theoretical developments described in Section 3, it suffices now to say that the quantum-like features of the walkers emerge at high memory, as arises when the Faraday threshold is approached.

2.2.1. Single-particle diffraction. The first evidence of the walker's quantum-like behavior was provided by Couder & Fort's (2006) study of walker diffraction through slits. In their single-slit study, walkers were directed, one at a time, toward a slit in a barrier (**Figure 3**). When walkers passed through the slit, they were diverted from their original path owing to the interaction between their pilot-wave field and the barrier. The authors directed 125 walkers toward the slit with uniform spatial density at normal incidence, providing the best approximation to an incident plane wave. The walker diffraction was quantified by the deflection angle α in the far field. The histogram for α was wavelike, with three peaks, and roughly consistent with the amplitude expected from the interference of a monochromatic wave with wavelength λ_F (**Figure 3b**). A qualitatively similar distribution was obtained with their simulations. This system represents a hydrodynamic analog of the single-photon diffraction experiments that constituted the doctoral thesis of G.I. Taylor (1909).
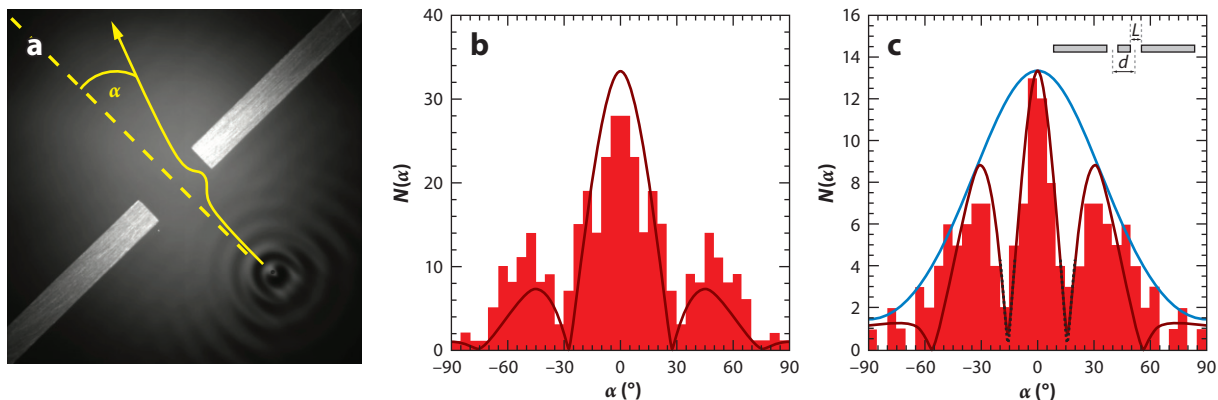
Figure 3

Single-particle diffraction. (*a*) A walker passing through a single slit. (*b*) The histogram for the deflection angle α from the single-slit experiments. (*c*) The histogram for α from the double-slit experiments. Figure adapted with permission from Couder & Fort (2006), courtesy of Yves Couder.

Couder & Fort's (2006) second study examined a hydrodynamic analog of the double-slit experiment with photons or electrons (Davisson & Germer 1927, Bach et al. 2013), the inscrutability of which is widely accepted (Feynman et al. 1964). A wavelike histogram for α emerged, roughly consistent with the amplitude of a monochromatic wave of wavelength λ_F diffracted by the double slit. The proposed mechanism is as follows. While the walker passes through one slit or the other, its guiding wave passes through both; thus, the walker effectively feels the second slit by virtue of its pilot wave. The feasibility of such an interaction, which relies on the spatial delocalization of the walker, is readily checked by comparing the decay time of the pilot wave to the walker's translation time.

Couder & Fort (2006) point out that, if one could not directly observe the walker, one might infer an uncertainty principle in position and momentum by virtue of the diffraction of the pilot wave. Thus, if an observer cannot ascertain the crossing point, he or she would be unable to predict the walker's final trajectory, hence the resulting uncertainty in momentum. An additional uncertainty might be inferred if one could not resolve the walker's bouncing phase, specifically when it is in contact with the bath and when it is in free flight. Given the complex interaction between the walker and its wave field as it passes through the slit, one expects its path to depend on this bouncing phase. Such a dependence is suggested by the apparent independence of α on the crossing point. The experiments of Couder & Fort (2006) indicate that the pilot-wave dynamics within the slit is sufficiently complex to be chaotic, with the deflection angle α sensitive to both the crossing point and the bouncing phase.

2.2.2. Tunneling. Eddi et al. (2009b) examined the interaction of a walker with barriers overlaid by a thin fluid layer. The incidence of the pilot-wave field on the barrier generates partial reflection and an evanescent tail that decays across the barrier. The reflected wave typically causes the reflection of an approaching walker; however, the drop-wave-barrier interaction occasionally permits the droplet to tunnel across. The tunneling probability decreases exponentially with the barrier width and increases as the Faraday threshold is approached. Once again, the quantum-like behavior (Gamow 1928) results from the pilot-wave dynamics, and the unpredictability is rooted in the complex interaction between the droplet and its spatially extended guiding wave.
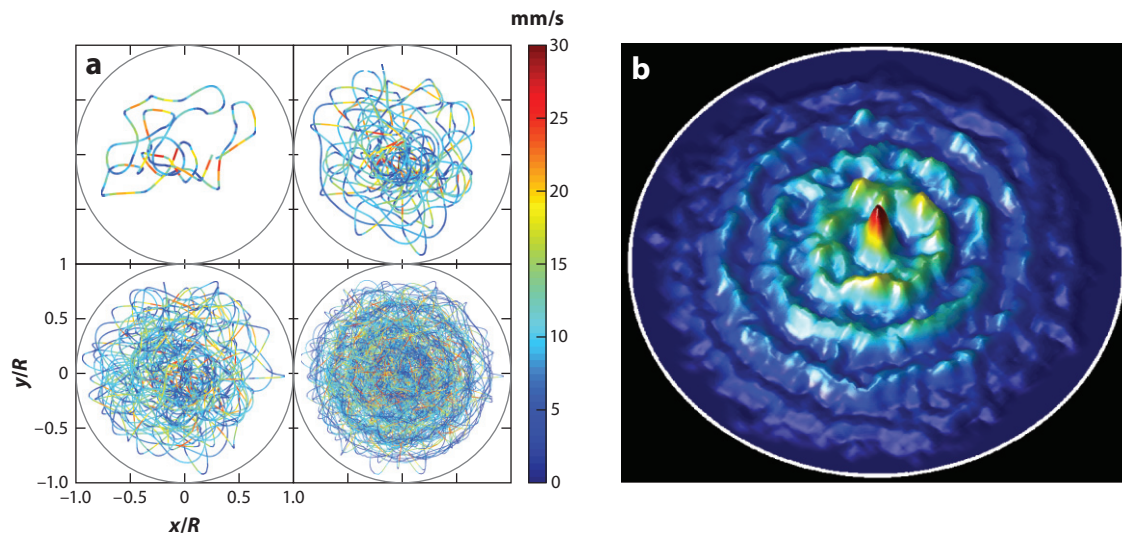
Figure 4

A walker in a circular corral of radius $R = 14.3$ mm. (*a*) Trajectories of increasing length in the high-memory regime are color coded according to droplet speed. (*b*) The histogram of the walking droplet's position corresponds roughly to the amplitude of the corral's Faraday wave mode. Figure adapted with permission from Harris et al. (2013). Copyright 2013, AIP Publishing LLC.

2.2.3. Motion in confined geometries. The second experimental arrangement in which a coherent statistical behavior was reported was for walkers in confined geometries, specifically circular corrals (Harris & Bush 2013, Harris et al. 2013) (see **Supplemental Video 1**; follow the **Supplemental Material link** from the Annual Reviews home page at **http://www. annualreviews.org**). At low memory, the walkers loop around the walls of the corral. As the memory is increased, progressively more complex orbits arise: wobbling circular orbits, drifting elliptical orbits, or epicycles. At very high memory, the trajectories become complex and presumably chaotic owing to the complexity of the wave field resulting from reflections off the boundaries (**Figure 4a**).

▶ Supplemental Material

The histogram presented in **Figure 4b** indicates the emergence of a coherent statistical behavior from this chaotic pilot-wave dynamics. The probability of finding a walker at a given point in the corral is roughly prescribed by the amplitude of the Faraday wave mode of the cavity at the prescribed forcing frequency. As was the case for single-particle diffraction (Couder & Fort 2006), the histogram has approximately the same wavelength as the pilot wave but a form prescribed by the system geometry. Because the corral was tuned to fit a single Faraday mode, the statistics might thus have been anticipated with no knowledge of the dynamics other than the guiding wavelength λ_F and the corral geometry. The observed statistical behavior is thus roughly analogous to that reported in the quantum corral experiments (Crommie et al. 1993a,b), in which the density of electrons trapped on a copper substrate was found to have a wavelike pattern with the de Broglie wavelength, λ_{dB}, and a form prescribed by the corral shape (Fiete & Heller 2003).

2.2.4. Motion in a rotating frame. An object moving horizontally with uniform speed u_0 in a frame rotating about a vertical axis with angular frequency Ω executes an inertial orbit of radius $r_i = u_0/2\Omega$, at which the inertial force mu_0^2/r_i is balanced by the Coriolis force $2m\Omega u_0$. Fort et al. (2010) examined walkers on a rotating, vibrating bath and characterized the dependence of the orbital radii r_o on Ω. In the low-memory regime, the walker's orbital radii decrease

Theoretical predictions
— Linearly stable
— Linearly unstable
— Linearly unstable oscillatory
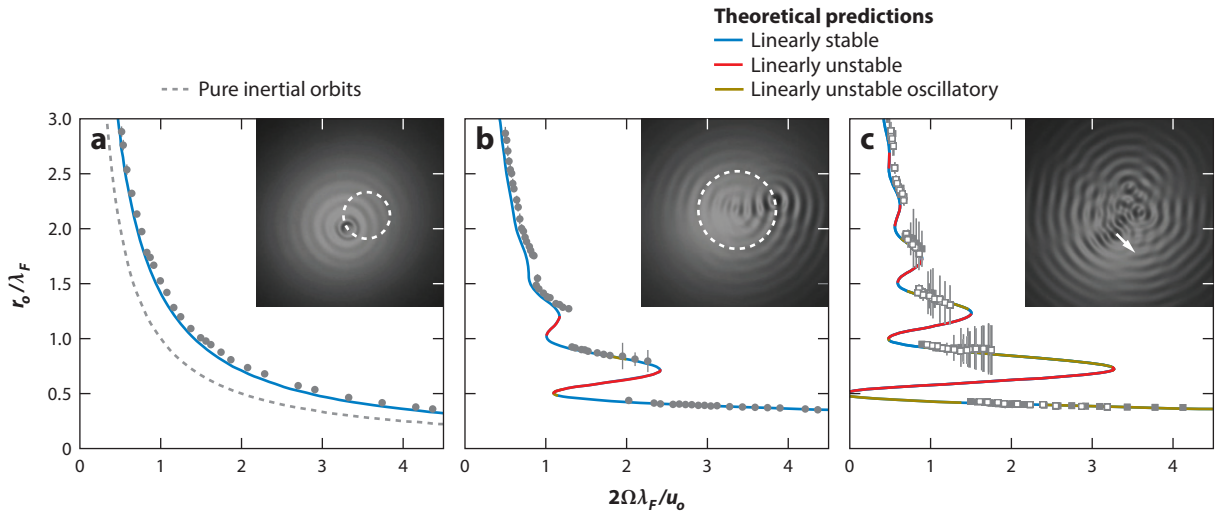
- - - Pure inertial orbits

Figure 5

Measured orbital radius r_o as a function of the bath's rotation rate Ω (Harris & Bush 2014a): (*a*) low memory ($\gamma/\gamma_F = 0.822$), (*b*) intermediate memory ($\gamma/\gamma_F = 0.954$), and (*c*) high memory ($\gamma/\gamma_F = 0.971$). The dashed curve in panel *a* indicates pure inertial orbits, $r_i = u_0/2\Omega$, the offset from which is prescribed by the droplet's hydrodynamic boost factor: $r_o = \gamma_B r_i$ (Bush et al. 2014). The solid curves are the theoretical predictions of Oza et al. (2014a). The blue segments are linearly stable, the red linearly unstable, and the dark yellow linearly unstable oscillatory branches. Data on the unstable dark yellow branches indicate the nonlinear stability of the wobbling states. Error bars denote wobbling amplitudes. Figure adapted with permission from Oza et al. (2014a).

monotonically with the rotation rate according to $r_o = c_o r_i$, where $c_o \approx 1.3$ is a fitting parameter. At high memory, r_o no longer varies continuously with Ω: Instead, certain orbital radii are forbidden. Orbital quantization then emerges through the walker's interaction with its own wake (**Figure 5**).

Because the Coriolis force $2m\dot{\mathbf{x}}_p \times \mathbf{\Omega}$ acts on a mass m in a rotating frame as does the Lorentz force $q\dot{\mathbf{x}}_p \times \mathbf{B}$ on a charge q in a uniform magnetic field $\mathbf{B}$ (Weinstein & Pounder 1945), Fort et al. (2010) proposed a correspondence between the quantized inertial orbits of walkers and the Landau levels of electrons. In the high-memory regime, the orbital radii are roughly quantized on the Faraday wavelength, just as Landau levels are quantized on the de Broglie wavelength. Eddi et al. (2012) further explored this correspondence by examining the influence of rotation on a pair of orbiting droplets. They found that the orbital radii increased or decreased according to whether the pair rotated in the same or opposite sense relative to the bath, indicating an analogy with Zeeman splitting of atomic energy levels.

The rotating system was revisited by Harris & Bush (2014a), who demonstrated that orbital quantization arises only for a limited range of forcing accelerations. The emergence of orbital quantization was detailed (**Figure 5**), along with the relatively rich behavior arising at higher memory. As the memory is increased progressively, the orbital states become unstable, giving way to wobbling orbital motions and then more complex periodic or aperiodic trajectories. In the high-memory limit, irregular chaotic trajectories emerge as the walker drifts between unstable orbits (**Figure 6**). The histogram of the trajectory's radius of curvature is characterized by a multimodal form, with peaks corresponding to the radii of the unstable orbits, which suggests their persistent dynamical influence.
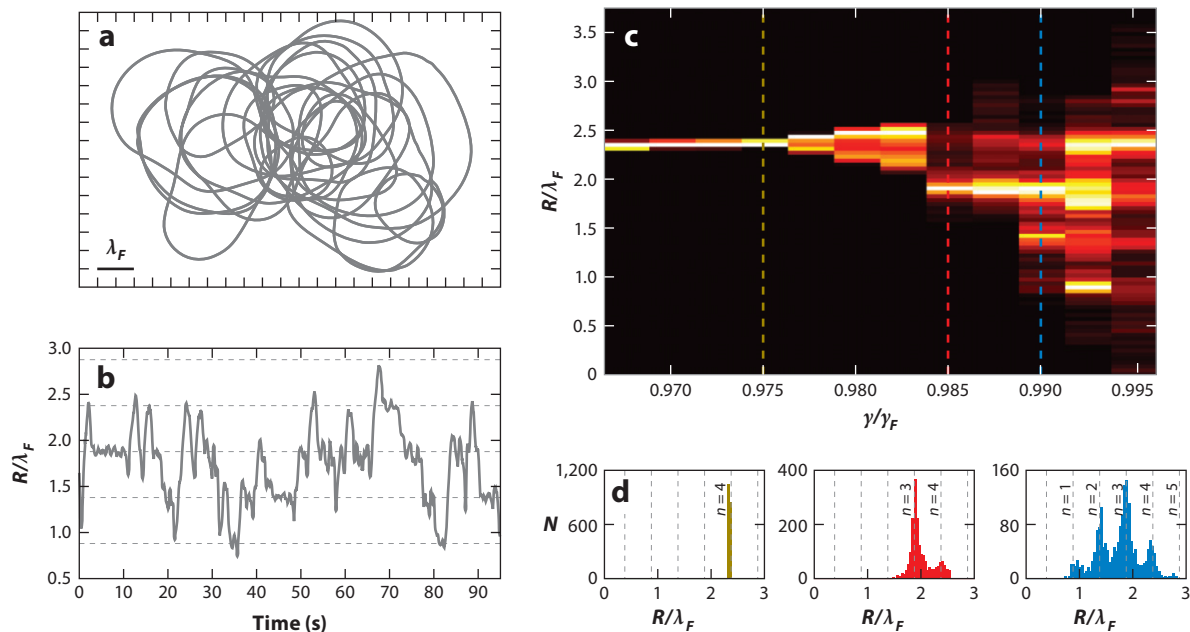
Figure 6

Chaotic walking in a frame rotating at $\Omega = 0.79$ rad/s. (*a*) Chaotic trajectory at high memory, $\gamma/\gamma_F = 0.990$. (*b*) Time trace of the radius of curvature R of the trajectory shown in panel *a*. (*c*) Probability distribution of R as a function of the vibrational forcing γ/γ_F. The brightness of a segment corresponds to the relative probability within a single column. (*d*) Histograms of the local radius of curvature along the three vertical columns indicated in panel *c* at $\gamma/\gamma_F = 0.975$ (*dark yellow*), 0.985 (*red*), and 0.990 (*blue*). The gray dashed vertical lines represent the zeros of the Bessel function $J_0(k_F r)$. Figure adapted with permission from Harris & Bush (2014a).

2.2.5. Motion in a central force. Couder's group has succeeded in encapsulating ferrofluids with silicone oil. The resulting two-component drops can walk just as do their homogeneous counterparts. By applying a vertical magnetic field with a radial gradient, Perrard et al. (2014a,b) examined the dynamics of walkers in the central force field resulting from a harmonic potential. In addition to circular orbits, more complex orbital states arose, including ovals, lemniscates, and trefoils, all of which may either be stationary or precess azimuthally. The authors characterized the resulting family of complex orbits in terms of the mean radius $\bar{R}$ and angular momentum $\bar{L}_z$ (**Figure 7**). The results indicate that the dynamic constraint imposed on the walker by its pilot-wave field imposes on its orbital states a double quantization in the mean energy and angular momentum.

Perrard et al. (2014b) presented a theoretical rationale for the quantized orbital states (or eigenstates) in terms of the energy landscape, specifically the wave field generated by the orbiting walker (see also M. Labousse, S. Perrard, Y. Couder & E. Fort, submitted manuscript). When the walker did not settle onto a pure eigenstate, it oscillated between nearby eigenstates, for example, an oval and a lemniscate. Thus, as was the case in the rotating walker system (Harris & Bush 2014a), complex trajectories emerged in the high-memory limit: The walker drifted between the system's unstable eigenstates, the result being multimodal statistics (Perrard et al. 2014a).

2.2.6. Bound states and other oddities. Pairs of bouncing drops may interact through their wave fields to form bound states (Protière et al. 2005). Likewise, crystalline structures may form from aggregates of nearly identical bouncers (**Figure 1d**). Lieber et al. (2007) reported both stationary
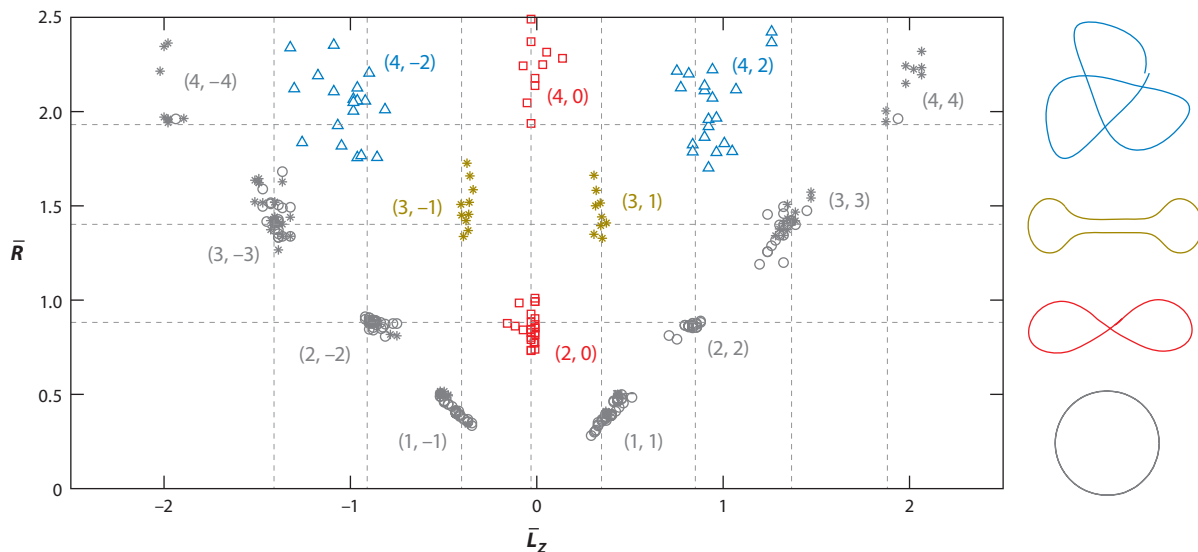
Figure 7

Double quantization for walkers in a central force field. Observed orbits include circles, lemniscates, dumbbells, and trefoils. Orbits are classified according to their mean radius $\bar{R} = \sqrt{\langle R^2 \rangle}/\lambda_F$ and angular momentum $\bar{L}_z = \langle L_z \rangle/(m\lambda_F u)$. Figure adapted with permission from Perrard et al. (2014b).

and spontaneously spinning lattices. Eddi et al. (2009a) achieved 8 of the 11 Archimedean tilings of the plane with arrays of bouncers, the stability of which was also examined (Eddi et al. 2011a). For pairs of bouncers of different size, the asymmetry of the resulting wave field may lead to self-propelling, ratcheting states (Eddi et al. 2008). Dynamic bound states may also arise from the interaction of walking droplets, their form depending on both the size and bouncing phase of the walkers (Protière et al. 2005). Protière et al. (2008) explored the exotic orbits arising from the interaction of walkers of different size. Pairs of identical walkers may scatter, lock into orbit, or translate together side by side in the promenade mode, in which the distance between them fluctuates periodically (C. Borghesi, J. Moukhtar, M. Labousse, A. Eddi, Y. Couder & E. Fort, submitted manuscript).

Gilet et al. (2008) and Dorbolo et al. (2008) examined the bouncing of relatively large oil drops ($D \sim 1.5$ mm, $v < 100$ cS) on a highly viscous bath ($v = 1,000$ cS). Levitation criteria were deduced, and nonaxisymmetric modes of droplet vibration excited, leading to propulsion via tumbling. More complex fluid topologies have also been explored. Terwagne et al. (2010) examined the bouncing of a two-phase droplet, elucidating the criterion for emulsification. Gier et al. (2012) studied the levitation of polymeric droplets. Pucci et al. (2011, 2013) examined the dynamics of a floating lens of alcohol on a vibrating bath of relatively viscous oil. When the lens becomes unstable to Faraday waves, the resulting radiation pressure may deform the lens, leading to striking static and dynamic forms.

3. THEORETICAL DEVELOPMENTS: AN EXPOSED VARIABLE THEORY

The charm of the hydrodynamic pilot-wave system is its accessibility: All the properties of the walker, the droplet and its guiding wave field, are visible. That is not to say that it is simply

described: The walker system is remarkably subtle, with its dynamical and statistical behavior strongly dependent on all the system parameters.

3.1. Bouncing Mechanics

Considerable effort has been devoted to elucidating the high–Reynolds number ($R_e = Ua/\nu$) impact of millimetric drops on solids (de Gennes et al. 2002, Yarin 2006). At small Bond number $B_o = \rho g a^2/\sigma$, surface tension dominates gravity, so a drop remains nearly spherical unless distorted by impact. For low–Weber number impacts, $W_e = \rho U^2 a^3/\sigma \ll 1$, the distortion is weak, and the drop behaves roughly like a linear spring with a spring constant proportional to σ (Okumura et al. 2003): During impact, kinetic energy is converted to surface energy, and then back to kinetic energy, with only a small viscous loss provided $R_e \gg 1$. Moláček & Bush (2012) demonstrated that for the parameter regime of walkers ($R_e \sim 20$, $B_o \sim 0.1$, $W_e \sim 0.1$), the distortion induced by impact on a rigid substrate may be described in terms of a family of quasi-static forms, and the collision dynamics in terms of a logarithmic spring.

The walkers are millimetric, and the principal force imparted to them during impact on the bath is associated with curvature rather than hydrostatic pressure. Thus, the dominant physics of impact is captured through the consideration of drop impact on a soap film, a configuration examined by Gilet & Bush (2009a,b), who demonstrated that the soap film acts on the drop like a linear spring, with a spring constant proportional to σ. Their investigation of a drop on a vibrating film revealed and rationalized a number of complex bouncing states. Drop impact on a vibrating fluid bath is complicated by the influence of the bath's inertia (Prosperetti & Oguz 1993).

To describe the impact of a bouncing drop on a vibrating liquid bath, Moláček & Bush (2013a,b) developed a hierarchy of models of increasing complexity, building on their model of impact on a rigid substrate (Moláček & Bush 2012) through consideration of the bath deformation. A logarithmic spring model again emerged, their model incorporating the measured logarithmic dependence of the coefficient of restitution C_R and contact time T_C on W_e. Although thus semiempirical, the resulting model has no free parameters. It correctly predicts the bouncing threshold, as well as the thresholds between the more energetic bouncing states (**Figure 2**). The bouncer must satisfy a resonance condition. For the (1, 1) bouncer, this is simply stated: The impact time plus the time of flight must equal the Faraday period. As γ increases progressively, the phase of impact changes continuously until the resonance condition can no longer be satisfied without the bouncer changing modes. For a description of the low-energy bouncing states, it was adequate to assume that the interface recovered to horizontal before the next impact. Modeling the more vigorous bouncing and walking states required consideration of the wave field.

Moláček & Bush (2013b) calculated the form of the wave field generated for the small-drop parameter regime of interest. Because a drop in the period-doubled bouncing state lands on the crest of its wave (Protière et al. 2006), it may be destabilized into a walking state. Modeling the resulting horizontal dynamics required the dependence of the coefficient of tangential restitution C_T on W_e, which was again deduced empirically. The resulting model successfully rationalized the observed walking thresholds (**Figure 2**), as well as the dependence of the walking speed on the system parameters (Moláček & Bush 2013b). Their study underscored the subtle role of impact phase on the walker dynamics: As the forcing acceleration is increased progressively, the impact phase shifts, and the walker may switch from one walking mode to another.

Terwagne et al. (2013) developed a relatively simple mass-spring-dashpot model of a droplet bouncing on a bath. Wind-Willassen et al. (2013) built upon the models of Moláček & Bush (2013a,b) to present the most complete study to date. New complex bouncing modes and different gaits arising within the walking regime were reported and rationalized (**Figure 2**). The dynamics of

droplets on a vibrating bath in the parameter regime relevant to walkers is now well characterized and understood. Existing regime diagrams provide a valuable resource for benchmarking new experimental studies.

3.2. Trajectory Equation

Protière et al. (2006) developed the first theoretical description of walking droplets. The model captures the essential physics of the problem, specifically the propulsion of the drop by virtue of a resonant interaction with a monochromatic wave field centered on the drop and generated at each impact. It reproduced several qualitative features of droplet behavior, including the bifurcation from bouncing to walking and the increase of walking speed with forcing acceleration. However, the model incorporated only the wave field of the most recent impact. A similar low-memory approximation was used to model walkers in corrals (Shirikoff 2013). Variable memory has been incorporated in Emmanuel Fort's numerical model, which has captured many features of the walker system, including single-particle diffraction (Couder & Fort 2006), quantized orbits (Fort et al. 2010), and doubly quantized orbits (Perrard et al. 2014a,b). This model provides a valuable exploratory tool that illustrates the critical role of memory on the walker dynamics; however, it does not capture the detailed dependence of the system on the fluid parameters.

Moláček & Bush (2013b) developed a hydrodynamically consistent equation of motion for a drop of mass m at a position $\mathbf{x}_p(t)$ walking in resonance with its wave field of shape $h(\mathbf{x}, t)$. By time averaging over the bouncing period, they eliminated the vertical dynamics from consideration and so deduced the trajectory equation:

$$m\ddot{\mathbf{x}}_p + D\dot{\mathbf{x}}_p = -mg\nabla h(\mathbf{x}_p, t). \tag{1}$$

The second term represents the time-averaged drag resulting from both flight and impact, with D being a drag coefficient that depends on the system parameters in a known fashion (Moláček & Bush 2013b). The third term is the propulsive wave force resulting from the drop's landing on an inclined surface. As $h(\mathbf{x}, t)$ depends on the history of the drop, so too does the wave force. The surface wave generated by a single impact may be approximated as a monochromatic radial Bessel function of the first kind, $J_0(k_F r)$ (Eddi et al. 2011b, Moláček & Bush 2013a, Oza et al. 2013), so the interface height generated by all previous bounces required for this time-averaged model is

$$h(\mathbf{x}, t) = A \sum_{n=-\infty}^{\lfloor t/T_F \rfloor} J_0(k_F |\mathbf{x} - \mathbf{x}_p(nT_F)|)e^{-(t-nT_F)/(T_F M)}. \tag{2}$$

The dimensionless memory parameter $M = T_d/[T_F(1 - \gamma/\gamma_F)]$ depends on the Faraday period T_F, the decay time of unforced waves T_d, and the proximity to the Faraday threshold γ_F (Eddi et al. 2011b). The wave amplitude A likewise depends in a known fashion on the system parameters, including the impact phase (Moláček & Bush 2013b). The wave force becomes increasingly important at high memory, as $\gamma \to \gamma_F$, when the waves are relatively persistent.

With a wave field in the form of the discrete sum (Equation 2), the trajectory equation shown in Equation 1 is difficult to analyze. Oza et al. (2013) demonstrated that, as the vertical dynamics is fast relative to the horizontal dynamics, one may approximate this sum by an integral. The resulting stroboscopic approximation yields the dimensionless trajectory equation

$$\kappa_0(1 - \Gamma)\ddot{\mathbf{x}}_p + \dot{\mathbf{x}}_p = \frac{2}{(1-\Gamma)^2} \int_{-\infty}^{t} \frac{J_1(|\mathbf{x}_p(t) - \mathbf{x}_p(s)|)}{|\mathbf{x}_p(t) - \mathbf{x}_p(s)|}(\mathbf{x}_p(t) - \mathbf{x}_p(s))e^{-(t-s)}ds. \tag{3}$$

This formulation includes two dimensionless parameters. The first, $\Gamma = (\gamma - \gamma_W)/(\gamma_F - \gamma_W)$, indicates the vigor of the forcing, the relative distance from the walking ($\Gamma = 0$) and Faraday

($\Gamma = 1$) thresholds. The second contains all the fluid parameters appearing in Equations 1 and 2: $\kappa_0 = (m/D)^{3/2} k_F \sqrt{gA/2T_F}$. The nonlocal form of the dynamics is apparent: The wave force acting on the walker is a function of its past, specifically its path, along which it lays down a field of Faraday waves.

The trajectory equation shown in Equation 3 describes the dynamics evident when the system is strobed at ω_F, when the walker appears to be pushed along continuously by its pilot-wave field (Harris & Bush 2013) (see **Supplemental Video 1**). Through its neglect of the vertical dynamics and impact phase, it is relatively amenable to analysis. Oza et al. (2013) showed that the stationary bouncing state $\dot{\mathbf{x}}_p = 0$ is stable until the walking threshold γ_w, beyond which steady walking solutions arise. The resulting theoretical predictions for both the walking threshold γ_w and the dependence of the walker speed on γ for $\gamma > \gamma_w$ adequately describe the existing data. The only fitting parameter in this strobed model is the impact phase, reasonable bounds on which are known from experiments (Moláček & Bush 2013b).

The trajectory equation shown in Equation 3 also yields insight into the stability of the walking state, the robustness of which is not obvious, given that the drop is riding the crest of its wave field. Linear stability analysis demonstrates that the walker is stable to colinear perturbations but is neutrally stable to transverse perturbations: If perturbed laterally from rectilinear motion, it will simply change course and proceed in a new direction (Oza et al. 2013). This result is consistent with the skittishness of the walker, the sensitivity of its path to perturbation, and its evidently chaotic motion in complex geometries, including corrals and slits.

3.3. Orbital Dynamics

The strobed model of Oza et al. (2013) has also allowed for an assessment of the stability of the quantized orbits in a rotating frame (Fort et al. 2010, Harris & Bush 2014a). To describe this configuration, the trajectory equation shown in Equation 3 is augmented by the Coriolis force. Circular orbital solutions with constant radius r_o and frequency ω_o are sought, and their linear stability assessed (Oza et al. 2014a). **Figure 5** illustrates the predicted dependence of the orbital radius on the rotation rate for three memory values. The predicted stability of orbits along the solution curves is indicated by their color. At low memory (**Figure 5a**), all circular orbits are stable, with orbital radii decreasing monotonically with Ω. At intermediate memory (**Figure 5b**), two unstable solution branches arise, corresponding to forbidden radii, the origins of the orbital quantization. At high memory (**Figure 5c**), the solution curve has linearly stable, linearly unstable, and linearly unstable oscillatory branches.

Numerical simulation of the trajectory equation has revealed the behavior of the walkers in the linearly unstable regions (Oza et al. 2014b). **Figure 8** summarizes the dependence of the orbital dynamics on γ/γ_F and the initial orbital radius r_o. As γ/γ_F is increased progressively, the stable circular orbits are typically succeeded by wobbling orbits with, in turn, stationary and translating orbital centers. In the high-memory limit, all but the smallest orbits become unstable, and chaotic trajectories arise. Although the trajectories are irregular, they exhibit coherent statistics. As in the experiments of Harris & Bush (2014a) (**Figure 6**), the walker has a tendency to follow arcs with radii of curvature corresponding to the unstable orbital states; thus, the histograms for the radius of curvature exhibit peaks at these radii, the number and relative magnitudes of which depend on the system memory. A coherent multimodal statistics thus emerges owing to the persistent dynamical influence of the unstable orbital states. These recent studies elucidate the origins of two key quantum-like behaviors, quantization and multimodal statistics, in orbital pilot-wave dynamics (Fort et al. 2010; Harris & Bush 2014a; Oza et al. 2014a,b; Perrard et al. 2014a,b; M. Labousse, S. Perrard, Y. Couder & E. Fort, submitted manuscript).
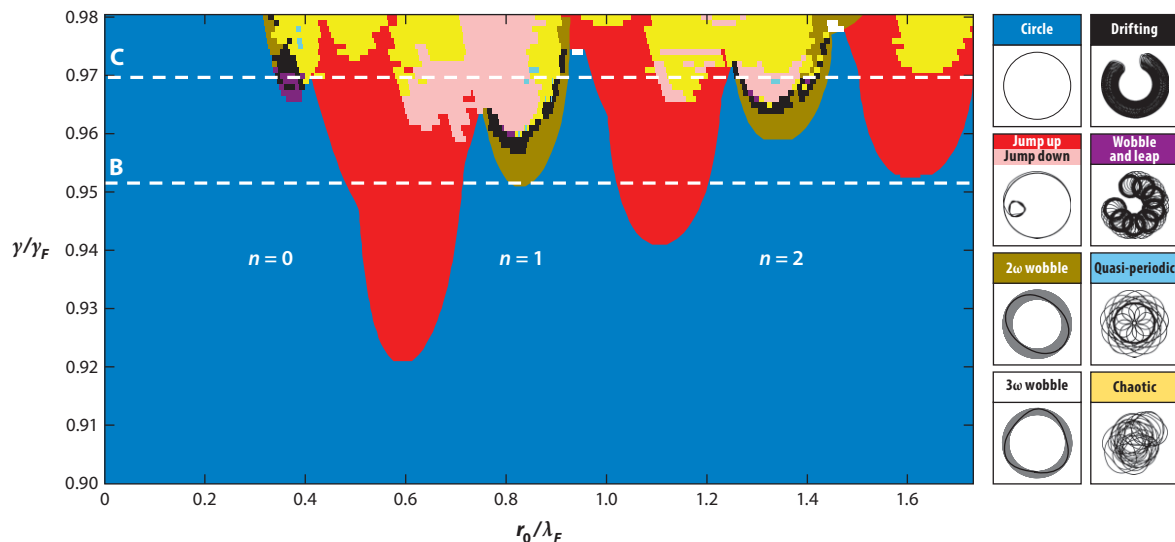
▶ Supplemental Material

Figure 8

Numerical simulations of walker trajectories in a rotating frame indicate the dependence of their form on the vibrational forcing γ/γ_F and the initial orbital radius r_o. Blue regions denote stable orbital regions, the boundaries of which are defined by the linear stability analysis of Oza et al. (2014a). Traverses B and C correspond to the solution curves illustrated in **Figure 5b,c**. Trajectories are color coded according to the legend. Note the windows of periodicity within the chaotic regime. Figure adapted with permission from Oza et al. (2014b). Copyright 2014, AIP Publishing LLC.

Another intriguing feature of the rotating system revealed through the analysis of Oza et al. (2014a) is the possibility of hydrodynamic spin states. As memory increases, the solution curves touch down on the $\Omega = 0$ axis (**Figure 5c**), indicating the existence of orbital solutions even in the absence of rotation. The wave force generated by the walker is then sufficient to balance the radial inertial force and so sustain its circular motion, a physical picture reminiscent of classical models of the electron (Schrödinger 1930, Burinskii 2008). When rotation is applied, as in the two-walker orbits of Eddi et al. (2012), a hydrodynamic analog of Zeeman splitting occurs. Although such hydrodynamic spin states are unstable in the parameter regime explored in our experiments, they are stable in other regions of the (κ_0, Γ) parameter space accessible in our more general pilot-wave framework (Equation 3).

An important conclusion of Harris & Bush (2014a) is that the statistics are extremely sensitive to all of the fluid parameters, their form changing drastically as γ/γ_F changes by as little as 1% (**Figure 6d**). Although the studies of single-particle diffraction (Couder & Fort 2006) and corrals (Harris et al. 2013) suggested that a unique Schrödinger-like wave function emerges in the high-memory limit (**Figures 3** and **4**), this relatively systematic study suggests otherwise. Rather, it is anticipated that a systematic reexamination of the diffraction and corral experiments will reveal multimodal statistics whose form will be strongly dependent on the system parameters.

3.4. Future Directions

The strobed model (Oza et al. 2013) successfully describes the motion of a single walker in unbounded domains. Having been benchmarked against the experiments of Harris & Bush (2014a), it is currently being applied to describe walker motion in central force fields, including harmonic and Coulomb potentials. A salient question is why the double quantization evident in the

harmonic potential (Perrard et al. 2014a,b; M. Labousse, S. Perrard, Y. Couder & E. Fort, submitted manuscript) was not apparent in the rotating system (Harris & Bush 2014a, Oza et al. 2014a,b). The principal shortcoming of the strobed model is that the wave field (Equation 2) does not incorporate the transient wave emitted during impact (Eddi et al. 2011b) and so cannot reliably capture the interaction of walkers with barriers (Eddi et al. 2009b, Harris et al. 2013, Carmignani et al. 2014) or other walkers (Protière et al. 2005, 2008; C. Borghesi, J. Moukhtar, M. Labousse, A. Eddi, Y. Couder & E. Fort, submitted manuscript). This shortcoming is being addressed in the next generation of pilot-wave models (P. Milewski, C. Galeano-Rios, A. Nachbin & J.W.M. Bush, submitted manuscript).

The theoretical developments have provided a more general framework for studying pilot-wave dynamics. In the stroboscopic model (Equation 3), only two dimensionless parameters appear. We have seen that certain quantum-like features, such as spin states, are unstable in the parameter regime accessible to this hydrodynamic pilot-wave system but are stable in others. The question then arises: For what values of (κ_0, Γ) does this generalized pilot-wave system exhibit behavior most reminiscent of quantum mechanics?

Fort & Couder (2013) took another intriguing step away from this hydrodynamic pilot-wave system and introduced the concept of an inertial walker. Whereas the real walker lays down a field of waves along its path, the inertial walker's wave field continues at the walker's velocity at the time of emission. For a discrete set of orbits, nonradiative resonant wave modes are excited; when circular, these orbits satisfy the Bohr-Sommerfeld quantization condition.

It is also interesting to consider how the walker motion might be described if the system were observed from above with no knowledge of the vibrational forcing, the bouncing, or the wave field. Labousse & Perrard (2014) highlighted the non-Hamiltonian features of the walker, describing its motion at low memory in terms of a Rayleigh oscillator. For a certain class of motions, Bush et al. (2014) demonstrated that the influence of the propulsive wave field and dissipation cancel to leading order, and the walker motion may be described in terms of the inviscid dynamics of a particle whose mass depends on its speed. They thus computed a hydrodynamic boost factor γ_B for the walker in terms of the system parameters: The effective inertial mass of a walker is $\gamma_B m$. This perspective rationalizes the anomalously large orbital radii evident in **Figure 5a** in terms of the walker's wave-induced added mass. Its value in more general settings is currently being explored.

4. RELATION TO QUANTUM MECHANICS

Realist interpretations of quantum mechanics assert that there is a real dynamics underlying the statistical description provided by standard quantum theory; thus, microscopic particles follow trajectories as do their classical counterparts (Bohr 1935, Einstein et al. 1935). This perspective suffered an early setback when von Neumann (1932) published a proof that erroneously suggested the impossibility of such a dynamics. It was over 30 years before Bell (1966) discredited von Neumann's and subsequent impossibility proofs. On such matters, I am inclined to give Bell (1987) the final word, to entertain the possibility of a real quantum dynamics underlying the well-established statistical theory. It is then only natural to ask what relation this hydrodynamic system might have to existing realist models of quantum dynamics.

4.1. The Madelung Transformation

The Madelung (1926) transformation allows the linear Schrödinger equation (LSE) to be recast in hydrodynamic form. Let us consider the standard quantum mechanical description of a particle of

mass m confined to a plane in the presence of a potential $V(\mathbf{x})$. Expressing the probability function in polar form, $\Psi(\mathbf{x}, t) = R(\mathbf{x}, t)e^{iS(\mathbf{x}, t)/\hbar}$, and substituting into the LSE, we obtain

$$\frac{D\rho_q}{Dt} + \rho_q \nabla \cdot \mathbf{v}_q = 0, \tag{4a}$$

$$\frac{\partial S}{\partial t} + \frac{1}{2}m\mathbf{v}_q^2 + Q + V = 0, \tag{4b}$$

where $\mathbf{v}_q(\mathbf{x}, t) = \nabla S(\mathbf{x}, t)/m$ is the quantum velocity of probability, $S(\mathbf{x}, t)$ is the action, $\rho_q(\mathbf{x}, t) = R^2$ is the probability density, and $Q(\mathbf{x}, t) = -(\hbar^2/2m)(1/R)\nabla^2 R$ is the quantum potential. Equation 4a indicates the conservation of probability, and Equation 4b corresponds to the quantum Hamilton-Jacobi equation. Taking the gradient of the latter yields the evolution equation for $\mathbf{v}_q$:

$$m\frac{D\mathbf{v}_q}{Dt} = -\nabla Q - \nabla V. \tag{5}$$

From the perspective of the fluid mechanician, the Madelung formulation (Equation 4) has two attractive features (Spiegel 1980). First, Planck's constant $\hbar$ appears only once, as the coefficient on the quantum potential. Second, the system corresponds to that describing the evolution of a shallow, inviscid fluid layer if one associates ρ_q with the fluid depth and $\mathbf{v}_q$ with the depth-averaged fluid velocity. When Q is linearized about a state of uniform ρ_q, it assumes the form of the curvature pressure in shallow-water hydrodynamics (Bühler 2010). One thus sees the relation between $\hbar$ in quantum statistics and surface tension σ in shallow-water hydrodynamics.

The Madelung transformation simply indicates that one can model quantum statistics hydrodynamically. For example, the statistics reported in the quantum corral experiments (Crommie et al. 1993a,b) might in principle be modeled with a Faraday wave system (see **Supplemental Video 1**) (Harris et al. 2013, Harris & Bush 2013). Specifically, provided the corrals can be tuned to fit a single mode, given the energy of the particle $E = \hbar\omega$, one can deduce the de Broglie wavelength, $\lambda_{dB} = 2\pi/k$, from the quantum dispersion relation $\omega = \hbar k^2/2m$, from which one might anticipate the probability distribution. Similarly, given the driving frequency, we know the Faraday wavelength from the water-wave dispersion relation (e.g., $\omega_F = \sqrt{\sigma/\rho}\, k_F^{3/2}$ for deep-water capillary waves), on the basis of which we might deduce the cavity's Faraday wave mode (**Figure 4b**). However, the corral experiments (Harris et al. 2013) indicate that one can also predict the statistics of walkers hydrodynamically; specifically, the histogram of a walker in a circular cavity is prescribed by the cavity's Faraday wave mode. Thus, in certain parameter regimes, walkers and quantum particles display similar statistical behavior, with the fluid properties (σ, ρ) standing in for ($\hbar, m$). What then can we make of the relation between walker motion and quantum dynamics?

4.2. Pilot-Wave Theories

The first pilot-wave theory was proposed by de Broglie (1923), who envisaged microscopic particles being guided by an accompanying wave field, pushed in a direction perpendicular to surfaces of constant phase (de Broglie 1926, 1930; Bacchiagaluppi & Valentini 2009). His original conception, his "double-solution theory" (de Broglie 1956), involved two waves, a real pilot wave centered on the particle and the statistical wave predicted by standard quantum theory. He asserted that quantum mechanics was intrinsically relativistic and proposed that the pilot wave originates in internal particle oscillations at the Compton frequency, $\omega_c = mc^2/\hbar$, at which rest mass energy is exchanged with wave energy. He proposed that the guiding wave field evolves according to the Klein-Gordon equation and consists of a monochromatic wave field in the particle's frame of

Supplemental Material

reference. The de Broglie relation, $p = \hbar k$, then relates the particle momentum to the de Broglie wavelength, $\lambda_{dB} = 2\pi/k$. Finally, he stressed the importance of the harmony of phases, by which the particle's internal vibration, seen as that of a clock, stays in phase with its guiding wave (de Broglie 1930, 1987). Thus, according to his conception, the wave and particle maintain a state of resonance.

Bohm (1952a,b) proposed a single-wave pilot-wave theory, according to which the guiding wave is precisely equivalent to the solution of Schrödinger's equation, and the particle velocity is identical to the quantum velocity of probability $\mathbf{v}_q$. Provided one takes an ensemble of initial conditions consistent with a solution to the LSE, the predictions of Bohmian mechanics are identical to those of standard quantum mechanics (Keller 1953). The result represented an important counterexample to the impossibility proofs of von Neumann (1932) and others that held sway at the time. Bohmian mechanics has since been developed substantially (Holland 1993, Towler 2009, Durr et al. 2012) and over time has been conflated with de Broglie's theory into what is now commonly referred to as the de Broglie–Bohm theory. The walking drop system suggests the potential value of disentangling these two pilot-wave theories.

The walker system is closer to de Broglie's double-solution theory than to Bohmian mechanics (Couder & Fort 2012). In the double-solution theory, as in this hydrodynamic system, the statistical wave must be augmented by the real pilot wave: The standard wave–particle duality must be extended to the wave–particle–pilot-wave trinity. The distinction is particularly evident in the corral geometry. According to Bohmian mechanics, the guiding wave is the statistical wave. In the walker system, conversely, the drop is piloted by the instantaneous wave field within the corral, whose form is relatively complex (Harris et al. 2013). Although both the real and statistical waves are characterized by the Faraday wavelength, the former is effectively centered on the particle and the latter is prescribed by the corral geometry (**Figure 4b**). The marked difference between the walker system and Bohmian mechanics is also evident in the diffraction experiments (Couder & Fort 2006). In quantum single-particle diffraction, Bohmian trajectories, as guided by the symmetric statistical wave, are necessarily symmetric: No particles cross the centerline (Philippidis et al. 1979). Conversely, the walker is guided by the complex pilot wave arising as it enters the gap. Its trajectory is complex, chaotic, and decidedly asymmetric: Walkers often cross the centerline. Although analog Bohmian trajectories could be defined for walkers on the basis of the statistics, they would simply represent ensemble averages of the real chaotic trajectories.

Table 1 compares de Broglie's double-solution theory and the walker system. Both systems are characterized by three timescales: a short time associated with a high-frequency oscillation, an intermediate time associated with the pilot-wave dynamics, and a long time over which the coherent statistics emerge (Harris & Bush 2013) (see **Supplemental Video 1**). Both systems are characterized by a single length scale that appears in both the dynamics and the statistics. The walker diffraction and corral experiments provide the first evidence that a particle-centered pilot-wave dynamics may give rise to a statistical wave with the same wavelength, but with a form prescribed by the bounding geometry.

De Broglie (1956) specified neither the physical origin nor the geometric form of his pilot wave. He proposed that it was linearly related to the statistical wave in the far field but was nonlinear (in an unspecified fashion) in the vicinity of the particle (de Broglie 1987). As he saw the particle as the source of the field, he invoked a singularity at the particle position. Three key features of the walker system are absent from de Broglie's conception. First, the walker interacts with an existing field (the interface) and so need not represent a singularity. Second, its monochromatic pilot-wave field is generated by parametric forcing. Third, the relation between the real and statistical waves emerges through chaotic pilot-wave dynamics.

▶ Supplemental Material

Table 1   A comparison among the walking droplet system, de Broglie's double-solution pilot-wave theory (de Broglie 1956, 1987), and its extension to stochastic electrodynamics (SED) (Kracklauer 1992, de la Peña & Cetto 1996, Haisch & Rueda 2000)

	Walkers	**de Broglie**	**SED pilot wave**
Pilot wave	Faraday capillary	Unspecified	Electromagnetic (EM)
Driving	Bath vibration	Internal clock	Vacuum fluctuations
Spectrum	Monochromatic	Monochromatic	Broad
Trigger	Bouncing	Zitterbewegung	Zitterbewegung
Trigger frequency	ω_F	$\omega_c = mc^2/\hbar$	$\omega_c = mc^2/\hbar$
Energetics	GPE $\leftrightarrow$ wave	$mc^2 \leftrightarrow \hbar\omega$	$mc^2 \leftrightarrow$ EM
Resonance	Droplet—wave	Harmony of phases	Unspecified
Dispersion $\omega(k)$	$\omega_F^2 \approx \sigma k^3/\rho$	$\omega^2 = \omega_c^2 + c^2 k^2$	$\omega = c k$
Carrier λ	λ_F	λ_{dB}	λ_c
Statistical λ	λ_F	λ_{dB}	λ_{dB}

In the walker system, energy is exchanged at ω_F between the drop's gravitational potential energy (GPE) and the capillary Faraday wave field. Zitterbewegung denotes particle oscillations at the Compton frequency ω_c.

4.3. Stochastic Electrodynamics

Soon after its inception (Bohm 1952a,b), Bohmian mechanics was extended to incorporate the influence of a stochastic subquantum realm (Bohm & Vigier 1954). According to this physical picture, stochastic particle motion underlies the quantum velocity of probability $\mathbf{v}_q$, the Madelung flow, just as Brownian motion underlies the streamlines within a fluid flow. This perspective, also pursued by de Broglie (1964) in his later years, led to a considerable literature (Goldstein 1987, Chebotarev 2000). Of particular interest is the result of Nelson (1966), who derived the LSE from consideration of a stochastic classical system, namely the Brownian motion of a mass m with diffusion coefficient $\hbar/(2m)$. A recent review of the successes and failures of the resulting stochastic interpretation of quantum mechanics is presented by Nelson (2012).

Stochastic electrodynamics (SED) posits a zero-point field (ZPF), electromagnetic vacuum fluctuations with an energy spectral form: $U(\omega) = \hbar\omega/2$ (Boyer 2011). Notably, these fluctuations represent a natural means of introducing Planck's constant $\hbar$ into a classical theory. SED has provided rationale for the Casimir effect, the stable ground state of the hydrogen atom (Cole & Zhou 2003), and the blackbody radiation spectrum (Boyer 2010). Surdin (1974) proposed the ZPF as a source of stochasticity in the subquantum realm. The resulting physical picture is being advanced: Grossing et al. (2012a,b) have taken inspiration from the bouncing droplets, referring to microscopic particles as bouncers.

De la Peña & Cetto (1996) suggested that vacuum fluctuations may generate a quantum particle's zitterbewegung (Schrödinger 1930, Hestenes 1990), specifically oscillations at the Compton frequency $\omega_c = mc^2/\hbar$. They further suggested that, as a particle translates, this vibrational motion interacts selectively with waves in the ambient vacuum field, a resonant interaction that amplifies an electromagnetic pilot wave. According to this physical picture, the carrier wave has the Compton wavelength $\lambda_c = 2\pi\hbar/mc$, and the de Broglie wavelength prescribes its modulation (Kracklauer 1992, 1999). This conception of a particle as a ZPF-driven oscillating charge with a resonance at ω_c has been further explored by Haisch & Rueda (2000), who suggested that it may offer insight into the origins of inertial mass, thereby linking the ZPF with the quantum wave nature of matter and relativistic mechanics (Haisch et al. 2001, Rueda & Haisch 2005). The

similarities between the resulting physical picture and the walker system are intriguing: The vacuum fluctuations would play the role of the vibrating bath in powering the system, with the particle's zitterbewegung that of the bouncing drop in triggering the pilot wave. This SED-based physical picture is also included in **Table 1**.

5. DISCUSSION

The hydrodynamic pilot-wave system discovered by Yves Couder, Emmanuel Fort, and coworkers is a fascinating new dynamical system in which a drop self-propels by virtue of a resonant interaction with its own wave field. It is the first macroscopic realization of a pilot-wave system of the form envisioned by de Broglie in his double-solution theory, and has extended the range of behaviors accessible to classical systems. It exhibits features reminiscent of quantum single-particle diffraction, tunneling, singly and doubly quantized orbits, orbital level splitting, spin, and multimodal statistics, all of which may be rationalized in terms of pilot-wave dynamics. Willful misinterpretation based on either intrusive measurement or impaired observation might lead to the inference of uncertainty relations and hydrodynamic boost factors. Likewise, exclusion principles might be inferred; for example, certain multiple-walker orbital states are forbidden by virtue of the fact that walkers must share the same wave field.

What features are critical to the quantum-like behavior? Quantization emerges from the dynamic constraint imposed on the walker by its monochromatic pilot-wave field. For example, quantized orbits may be understood in terms of the interaction of the walker with its own wake: Quantization emerges only when the wave field lasts longer than the orbital period. The dispersion relation of the wave field is not important. What is important is that the wave be monochromatic, hence the critical importance of the Faraday forcing and the resonance between the bouncing drop and its pilot wave. Studies of orbital motion suggest that multimodal statistics are a generic feature of chaotic pilot-wave dynamics: Unstable eigenstates serve as attractors that leave an imprint on the statistics. The general validity of this perspective needs to be explored through further examination of walkers in corrals (T. Gilet, submitted manuscript), single-particle diffraction, and entirely new geometries. Characterizing the transitions to chaos in this new pilot-wave system poses an exciting challenge to the dynamical systems community. The influence of stochastic forcing on this chaotic pilot-wave dynamics is also of considerable interest. Such a forcing may arise naturally in the laboratory through the influence of air currents or when the drop is in a chaotic walking state, and might be imposed in a controlled fashion through noise in the vibrational forcing.

The hydrodynamic system has numerous limitations as a quantum analog; however, some may be circumvented. Although the experiments can capture only two-dimensional pilot-wave dynamics, the attendant theoretical developments can be generalized to three dimensions. The wavelength of the walker's pilot wave is imposed by the frequency of the vibrational forcing and is independent of its speed; conversely, in quantum mechanics, the de Broglie relation, $p = \hbar k$, dictates a speed-dependent de Broglie wavelength. Such a dependence could be incorporated into existing pilot-wave models. Finally, we have seen that intrusive measurement, a defining feature of quantum mechanics, can be artificially imposed on the walker system. The question remains open as to whether some combination of intrusive measurement and chaotic pilot-wave dynamics might give rise to a hydrodynamic analog of entanglement.

Bell (1987) championed the de Broglie–Bohm pilot-wave theory on the grounds that it presents a conceptual framework for a mechanistic understanding of quantum dynamics, a framework that a purely statistical theory cannot possibly provide. Whatever its shortcomings and limitations, the new physical picture suggested by the walkers, that of a relatively complex chaotic pilot-wave

dynamics, also has this appealing feature. Moreover, it has precursors in a continuous arc of literature that leads back to de Broglie and Einstein, both of whom sought to reconcile quantum mechanics and relativity through consideration of the wave nature of matter (Bohm & Hiley 1982, Chebotarev 2000). The relation among this physical picture, quantum chaos (Gutzwiller 1990), and quantum field theory (Weinberg 1995) is left to the interested reader.

And lest the longevity of the quantum paradoxes be mistaken for their insurmountability, fluid mechanics has a cautionary tale to tell. In 1749, d'Alembert's paradox indicated that an object moving through an inviscid fluid experiences no drag, a prediction that was clearly at odds with experiments on high–Reynolds number gas flows. The result was a longstanding rift between experimentalists and theorists: For much of the nineteenth century, the former worked on phenomena that could not be explained, and the latter on those that could not be observed (Lighthill 1956). D'Alembert's paradox stood for over 150 years, until Prandtl's developments (Anderson 2005) allowed for the resolution of the dynamics on the hitherto hidden scale of the viscous boundary layer.

Finally, as concerns my alignment vis-à-vis quantum interpretations, I remain steadfastly agnostic; however, if forced to choose, I would be inclined to back, by virtue of its inclusivity, the logical extension of the Many-Worlds interpretation (Everett 1957), the Many-Many-Worlds interpretation, according to which each quantum interpretation is realized in some edition of the multimultiverse, and there is even one world in which there is only one world, a world in which quantum statistics are underlaid by chaotic pilot-wave dynamics, there is no philosophical schism between large and small, and beables be.

DISCLOSURE STATEMENT

ACKNOWLEDGMENTS

LITERATURE CITED

Anderson JD. 2005. Ludwig Prandtl's boundary layer. *Phys. Today* 58:45–48

Bacchiagaluppi G, Valentini A. 2009. *Quantum Theory at the Crossroads: Reconsidering the 1927 Solvay Conference.* Cambridge, UK: Cambridge Univ. Press

Bach R, Pope D, Liou S, Batelaan H. 2013. Controlled double-slit electron diffraction. *New J. Phys.* 15:033018

Bechhoeffer J, Ego V, Manneville S, Johnson B. 1995. An experimental study of the onset of parametrically pumped surface waves in viscous fluids. *J. Fluid Mech.* 288:325–50

Bell JS. 1966. On the problem of hidden variables in quantum mechanics. *Rev. Mod. Phys.* 38:447–52

Bell JS. 1982. On the impossible pilot wave. *Found. Phys.* 12:989–99

Bell JS. 1987. *Speakable and Unspeakable in Quantum Mechanics.* Cambridge, UK: Cambridge Univ. Press

Benjamin TB, Ursell F. 1954. The stability of the plane free surface of a liquid in vertical periodic motion. *Proc. R. Soc. Lond. A* 225:505–15

Berry MV, Chambers RG, Large MD, Upstill C, Walmsley JC. 1980. Wavefront dislocations in the Aharanov-Bohm effect and its water wave analogue. *Eur. J. Phys.* 1:154–62

Bohm D. 1952a. A suggested interpretation of the quantum theory in terms of hidden variables, I. *Phys. Rev.* 85:166–79

Bohm D. 1952b. A suggested interpretation of the quantum theory in terms of hidden variables, II. *Phys. Rev.* 85:180–93

Bohm D, Vigier JP. 1954. Model of the causal interpretation of quantum theory in terms of a fluid with irregular fluctuations. *Phys. Rev.* 96:208–16

Bohm D, Hiley BJ. 1982. The de Broglie pilot wave theory and the further development of new insights arising out of it. *Found. Phys.* 12:1001–16

Bohr N. 1935. Can quantum-mechanical description of physical reality be considered complete? *Phys. Rev.* 48:696–702

Boyer TH. 2010. Derivation of the Planck spectrum for relativistic classical scalar radiation from thermal equilibrium in an accelerating frame. *Phys. Rev. D* 81:105024

Boyer TH. 2011. Any classical description of nature requires classical electromagnetic zero-point radiation. *Am. J. Phys.* 79:1163–67

Bühler O. 2010. Wave-vortex interactions in fluids and superfluids. *Annu. Rev. Fluid Mech.* 42:205–28

Burinskii A. 2008. The Dirac-Kerr-Newman electron. *Gravit. Cosmol.* 14:109–22

Bush JWM. 2010. Quantum mechanics writ large. *Proc. Natl. Acad. Sci. USA* 107:17455–56

Bush JWM, Oza A, Moláček J. 2014. The wave-induced added mass of walking droplets. *J. Fluid Mech.* 755:R7. doi: 10.1017/jfm.2014.459

Carmigniani R, Lapointe S, Symon S, McKeon BJ. 2014. Influence of a local change of depth on the behavior of walking oil drops. *Exp. Thermal Fluid Sci.* 54:237–46

Chebotarev L. 2000. Introduction: the de Broglie-Bohm-Vigier approach in quantum mechanics. In *Jean-Pierre Vigier and the Stochastic Interpretation of Quantum Mechanics*, ed. S Jeffers, B Lehnert, N Abramson, L Chebotarev, pp. 1–18. Montreal: Apeiron

Cole DC, Zhou Y. 2003. Quantum mechanical ground state of hydrogen obtained from classical electrodynamics. *Phys. Lett. A* 317:14–20

Coste C, Lund F, Umeki M. 1999. Scattering of dislocated wave fronts by vertical vorticity and the Aharonov-Bohm effect. I. Shallow water. *Phys. Rev. E* 60:4908–16

Couder Y, Fort E. 2006. Single particle diffraction and interference at a macroscopic scale. *Phys. Rev. Lett.* 97:154101

Couder Y, Fort E. 2012. Probabilities and trajectories in a classical wave-particle duality. *J. Phys. Conf. Ser.* 361:012001

Couder Y, Fort E, Gautier C-H, Boudaoud A. 2005a. From bouncing to floating: noncoalescence of drops on a fluid bath. *Phys. Rev. Lett.* 94:177801

Couder Y, Protière S, Fort E, Boudaoud A. 2005b. Walking and orbiting droplets. *Nature* 437:208

Crommie MF, Lutz CP, Eigler DM. 1993a. Confinement of electrons to quantum corrals on a metal surface. *Science* 262:218–20

Crommie MF, Lutz CP, Eigler DM. 1993b. Imaging standing waves in a two-dimensional electron gas. *Nature* 363:524–27

Davisson C, Germer LH. 1927. The scattering of electrons by a single crystal of nickel. *Nature* 119:558–60

de Broglie L. 1923. Ondes et quanta. *C. R.* 177:507–10

de Broglie L. 1926. *Ondes et mouvements*. Paris: Gautier-Villars

de Broglie L. 1930. *An Introduction to the Study of Wave Mechanics*. London: Methuen & Co.

de Broglie L. 1956. *Une interprétation causale et nonlinéaire de la Mechanique ondulatoire: la théorie de la double solution*. Paris: Gautier-Villars

de Broglie L. 1964. La thermodynamique cachée des particules. *Ann. Inst. Henri Poincaré* 1:1–19

de Broglie L. 1987. Interpretation of quantum mechanics by the double solution theory. *Ann. Fond. Louis Broglie* 12:1–23

de Gennes PG, Brochard-Wyart F, Quéré D. 2002. *Gouttes, bulles, perles et ondes*. Paris: Belin

de la Peña L, Cetto AM. 1996. *The Quantum Dice: An Introduction to Stochastic Electrodynamics*. Dordrecht: Kluwer Acad.

Denardo BC, Puda JJ, Larraza A. 2009. A water wave analog of the Casimir effect. *Am. J. Phys.* 77:1095–101

Donnelly RJ. 1993. Quantized vortices and turbulence in helium II. *Annu. Rev. Fluid Mech.* 25:327–71

Dorbolo S, Terwagne D, Vandewalle N, Gilet T. 2008. Resonant and rolling droplets. *New J. Phys.* 10:113021

Douady S. 1990. Experimental study of the Faraday instability. *J. Fluid Mech.* 221:383–409

Durr D, Goldstein S, Zanghi N. 2012. *Quantum Physics Without Quantum Philosophy*. New York: Springer

Eddi A, Boudaoud A, Couder Y. 2011a. Oscillating instability in bouncing drop crystals. *Europhys. Lett.* 94:20004

Eddi A, Decelle A, Fort E, Couder Y. 2009a. Archimedean lattices in the bound states of wave interacting particles. *Europhys. Lett.* 87:56002

Eddi A, Fort E, Moisy F, Couder Y. 2009b. Unpredictable tunneling of a classical wave-particle association. *Phys. Rev. Lett.* 102:240401

Eddi A, Moukhtar J, Perrard J, Fort E, Counder Y. 2012. Level splitting at a macroscopic scale. *Phys. Rev. Lett.* 108:264503

Eddi A, Sultan E, Moukhtar J, Fort E, Rossi M, Couder Y. 2011b. Information stored in Faraday waves: the origin of path memory. *J. Fluid Mech.* 674:433–63

Eddi A, Terwagne D, Fort E, Couder Y. 2008. Wave propelled ratchets and drifting rafts. *Europhys. Lett.* 82:44001

Edwards WS, Fauve S. 1994. Patterns and quasi-patterns in the Faraday experiment. *J. Fluid Mech.* 278:123–48

Einstein A, Podolsky B, Rosen N. 1935. Can quantum-mechanical description of physical reality be considered complete? *Phys. Rev.* 47:777–80

Everett H. 1957. Relative state formulation of quantum mechanics. *Rev. Mod. Phys.* 29:454–62

Faraday M. 1831. On the forms and states of fluids on vibrating elastic surfaces. *Philos. Trans. R. Soc. Lond.* 121:319–40

Feynman RP, Leighton RB, Sands M. 1964. *The Feynman Lectures on Physics*. New York: Addison-Wesley

Fiete GA, Heller EJ. 2003. Theory of quantum corrals and quantum mirages. *Rev. Mod. Phys.* 75:933–48

Fort E, Couder Y. 2013. Trajectory eigenmodes of an orbiting wave source. *Europhys. Lett.* 102:16005

Fort E, Eddi A, Boudaoud A, Moukhtar J, Couder Y. 2010. Path-memory induced quantization of classical orbits. *Proc. Natl. Acad. Sci. USA* 107:17515–20

Gamow G. 1928. The theory of nuclear disintegration. *Nature* 122:805–7

Gier S, Dorbolo S, Terwagne D, Vandewalle N, Wagner C. 2012. Bouncing of polymeric droplets on liquid interfaces. *Phys. Rev. E* 86:066314

Gilet T, Bush JWM. 2009a. Chaotic bouncing of a drop on a soap film. *Phys. Rev. Lett.* 102:014501

Gilet T, Bush JWM. 2009b. The fluid trampoline: droplets bouncing on a soap film. *J. Fluid Mech.* 625:167–203

Gilet T, Bush JWM. 2012. Droplets bouncing on a wet, inclined surface. *Phys. Fluids* 24:122103

Gilet T, Terwagne D, Vandewalle N, Dorbolo S. 2008. Dynamics of a bouncing droplet onto a vertically vibrated interface. *Phys. Rev. Lett.* 100:167802

Gilet T, Vandewalle N, Dorbolo S. 2007. Controlling the partial coalescence of a droplet on a vertically vibrated bath. *Phys. Rev. E* 76:035302

Goldman DI. 2002. *Pattern formation and fluidization in vibrated granular layers, and grain dynamics and jamming in a water fluidized bed*. PhD Thesis, Univ. Tex., Austin

Goldstein S. 1987. Stochastic mechanics and quantum theory. *J. Stat. Phys.* 47:645–67

Grossing G, Fussy S, Mesa Pascasio J, Schwabl H. 2012a. An explanation of interference effects in the double slit experiment: classical trajectories plus ballistic diffusion caused by zero-point fluctuations. *Ann. Phys.* 327:421–27

Grossing G, Fussy S, Mesa Pascasio J, Schwabl H. 2012b. The quantum as an emergent system. *J. Phys. Conf. Ser.* 361:021008

Gutzwiller MC. 1990. *Chaos in Classical and Quantum Mechanics*. Berlin: Springer-Verlag

Haisch B, Rueda A. 2000. On the relation between a zero-point-field-induced inertial effect and the Einstein–de Broglie formula. *Phys. Rev. A* 268:224–27

Haisch B, Rueda A, Dobyns Y. 2001. Inertial mass and the quantum vacuum fields. *Phys. Rev. A* 268:224–27

Harris DM, Bush JWM. 2013. The pilot-wave dynamics of walking droplets. *Phys. Fluids* 25:091112

Harris DM, Bush JWM. 2014a. Droplets walking in a rotating frame: from quantized orbits to multimodal statistics. *J. Fluid Mech.* 739:444–64

Harris DM, Bush JWM. 2014b. Generating uniaxial vibration with an electrodynamic shaker and external air bearing. *J. Sound Vib.* In press

Harris DM, Moukhtar J, Fort E, Couder Y, Bush JWM. 2013. Wavelike statistics from pilot-wave dynamics in a circular corral. *Phys. Rev. E* 88:011001

Hestenes D. 1990. The zitterbewegung interpretation of quantum mechanics. *Found. Phys.* 20:1213–32

Holland PR. 1993. *The Quantum Theory of Motion: An Account of the De Broglie–Bohm Causal Interpretation of Quantum Mechanics*. Cambridge, UK: Cambridge Univ. Press

Jayaratne OW, Mason BJ. 1964. The coalescence and bouncing of water drops at an air-water interface. *Proc. R. Soc. Lond. A* 280:545–65

Keller J. 1953. Bohm's interpretation of the quantum theory in terms of "hidden" variables. *Phys. Rev.* 89:1040–41

Kracklauer AF. 1992. An intuitive paradigm for quantum mechanics. *Phys. Essays* 5:226–34

Kracklauer AF. 1999. Pilot wave steerage: a mechanism and test. *Found. Phys. Lett.* 12:441–53

Kumar K. 1996. Parametric instability of the interface between two fluids. *Proc. R. Soc. Lond. A* 452:1113–26

Kumar K, Tuckerman LS. 1994. Parametric instability of the interface between two fluids. *J. Fluid Mech.* 279:49–68

Labousse M, Perrard S. 2014. Non-Hamiltonian features of a classical pilot-wave dynamics. *Phys. Rev. E* 90:022913

Lieber SI, Hendershott MC, Pattanaporkratana A, Maclennan JE. 2007. Self-organization of bouncing oil drops: two-dimensional lattices and spinning clusters. *Phys. Rev. E* 75:056308

Lighthill J. 1956. Physics of gas flow at very high speeds. *Nature* 178:343–45

Madelung E. 1926. Quantentheorie in Hydrodynamischen form. *Z. Phys.* 40:322–26

Miles J, Henderson D. 1990. Parametrically forced surface waves. *Annu. Rev. Fluid Mech.* 22:143–65

Moisy F, Rabaud M, Salsac K. 2009. A synthetic Schlieren method for the measurement of the topography of a liquid interface. *Exp. Fluids* 46:1021–36

Moláček J, Bush JWM. 2012. A quasi-static model of drop impact. *Phys. Fluids* 24:127103

Moláček J, Bush JWM. 2013a. Droplets bouncing on a vibrating fluid bath. *J. Fluid Mech.* 727:582–611

Moláček J, Bush JWM. 2013b. Droplets walking on a vibrating fluid bath: towards a hydrodynamic pilot-wave theory. *J. Fluid Mech.* 727:612–47

Neitzel GP, Dell'Aversana P. 2002. Noncoalescence and nonwetting behavior of liquids. *Annu. Rev. Fluid Mech.* 34:267–89

Nelson E. 1966. Derivation of the Schrödinger equation from Newtonian mechanics. *Phys. Rev.* 150:1079–85

Nelson E. 2012. Review of stochastic mechanics. *J. Phys. Conf. Ser.* 361:012011

Newton I. 1979. *Opticks: Or a Treatise of the Reflections, Refractions, Inflections and Colours of Light*. Mineola, NY: Dover

Okumura K, Chevy F, Richard D, Quéré D, Clanet C. 2003. Water spring: a model for bouncing drops. *Europhys. Lett.* 62:237–43

Oza A, Harris DM, Rosales RR, Bush JWM. 2014a. Pilot-wave dynamics in a rotating frame: on the emergence of orbital quantization. *J. Fluid Mech.* 744:404–29

Oza A, Rosales RR, Bush JWM. 2013. A trajectory equation for walking droplets: a hydrodynamic pilot-wave theory. *J. Fluid Mech.* 737:552–70

Oza A, Wind-Willassen Ø, Harris DM, Rosales RR, Bush JWM. 2014b. Pilot-wave hydrodynamics in a rotating frame: exotic orbits. *Phys. Fluids* 26:082101

Perrard S, Labousse M, Fort E, Couder Y. 2014a. Chaos driven by interfering memory. *Phys. Rev. Lett.* 113:104101

Perrard S, Labousse M, Miskin M, Fort E, Couder Y. 2014b. Self-organization into quantized eigenstates of a classical wave-driven particle. *Nat. Commun.* 5:3219

Philippidis C, Dewdney C, Hiley BJ. 1979. Quantum interference and the quantum potential. *Nuovo Cimento* 52B:15–28

Pitaevskii L, Stringari S. 2003. *Bose-Einstein Condensation*. New York: Oxford Univ. Press

Prosperetti A, Oguz HN. 1993. The impact of drops on liquid surfaces and the underwater noise of rain. *Annu. Rev. Fluid Mech.* 25:577–602

Protière S, Bohn S, Couder Y. 2008. Exotic orbits of two interacting wave sources. *Phys. Rev. E* 78:036204

Protière S, Boudaoud A, Couder Y. 2006. Particle wave association on a fluid interface. *J. Fluid Mech.* 554:85–108

Protière S, Couder Y, Fort E, Boudaoud A. 2005. The self-organization of capillary wave sources. *J. Phys. Condens. Matter* 17:S3529–35

Pucci G, Ben Amar M, Couder Y. 2013. Faraday instability in floating liquid lenses: the spontaneous mutual adaptation due to radiation pressure. *J. Fluid Mech.* 725:402–27

Pucci G, Fort E, Ben Amar M, Couder Y. 2011. Mutual adaptation of a Faraday instability pattern with its flexible boundaries in floating fluid drops. *Phys. Rev. Lett.* 106:024503

Reynolds O. 1886. On the theory of lubrication. *Philos. Trans. R. Soc. Lond. A* 177:157–234

Rueda A, Haisch B. 2005. Gravity and the quantum vacuum inertia hypothesis. *Ann. Phys.* 14:479–98

Schrödinger E. 1930. Uber die kraftefreie Bewegung in der relativistischen Quantenmechanik. *Sitz. Preuss. Akad. Wiss. Phys. Math. Kl.* 24:418–28

Shirikoff D. 2013. Bouncing droplets on a billiard table. *Chaos* 23:013115

Spiegel E. 1980. Fluid dynamical form of the linear and nonlinear Schrödinger equations. *Physica D* 1:236–40

Surdin M. 1974. L'éctrodynamique stochastique et l'interprétation de la Mécanique Quantique. *C. R. Acad. Sci. Paris B* 278:881–83

Taylor GI. 1909. Interference fringes with feeble light. *Proc. Camb. Philos. Soc.* 15:114–15

Terwagne D. 2012. *Bouncing droplets, the role of deformations*. PhD Thesis, Univ. Liège

Terwagne D, Gilet T, Vandewalle N, Dorbolo S. 2009. Metastable bouncing droplets. *Phys. Fluids* 21:054103

Terwagne D, Gilet T, Vandewalle N, Dorbolo S. 2010. From a bouncing compound drop to a double emulsion. *Langmuir* 26:11680–85

Terwagne D, Ludewig F, Vandewalle N, Dorbolo S. 2013. The role of droplet deformations in the bouncing droplet dynamics. *Phys. Fluids* 25:122101

Terwagne D, Vandewalle N, Dorbolo S. 2007. Lifetime of a bouncing droplet. *Phys. Rev. E* 76:056311

Towler M. 2009. *De Broglie-Bohm pilot-wave theory and the foundations of quantum mechanics: a graduate lecture course*. Univ. Camb. **http://www.tcm.phy.cam.ac.uk/~mdt26/pilot_waves.html**

von Neumann J. 1932. *Mathematische Grundlagen der Quantenmechanik*. Berlin: Springer

Walker J. 1978. Drops of liquid can be made to float on the liquid. What enables them to do so? *Sci. Am.* 238:151–58

Weinberg S. 1995. *The Quantum Theory of Fields*, Vol. I: *Foundations*. Cambridge, UK: Cambridge Univ. Press

Weinstein A, Pounder JR. 1945. An electromagnetic analogy in mechanics. *Am. Math. Mon.* 52:434–38

Wind-Willassen Ø, Moláček J, Harris DM, Bush JWM. 2013. Exotic states of bouncing and walking droplets. *Phys. Fluids* 25:082002

Yang AL, Chien W, King M, Grosshandler WL. 1997. A simple piezoelectric droplet generator. *Exp. Fluids* 23:445–47

Yarin AL. 2006. Drop impact dynamics: splashing, spreading, receding, bouncing. *Annu. Rev. Fluid Mech.* 38:159–92

Young T. 1804. The Bakerian Lecture: experiments and calculations relative to physical optics. *Philos. Trans. R. Soc. Lond.* 94:1–16

Contents

Indexes

Errata

An online log of corrections to *Annual Review of Fluid Mechanics* articles may be found at http://www.annualreviews.org/errata/fluid